Polymer Journal (2018) 50:231–237
https://doi.org/10.1038/s41428-017-0010-x

ORIGINAL ARTICLE

Difference in dilute aqueous solution behavior between poly(ethylene glycol) and poly(ethylene oxide)

Akihisa Nakamura[1] · Yutaka Aoki[1] · Masashi Osa[2] · Daichi Ida[1] · Takenao Yoshizaki[1]

Received: 24 August 2017 / Revised: 27 September 2017 / Accepted: 22 October 2017 / Published online: 14 December 2017

Abstract

Static light scattering behavior was examined for poly(ethylene glycol) (PEG) and poly(ethylene oxide) (PEO) of small weight-average molecular weight M_w (3×10^3–2×10^4), in methanol and water at 25.0 °C, the former polymer having hydroxy groups at both ends and the latter having a methoxy group at one end and a hydroxy group at the other. It was found that some aggregates of large size are formed in aqueous solutions of the PEO samples with $M_w = 3.81 \times 10^3$ and 7.00×10^3, while all PEG and PEO samples are isolated in methanol solutions, and the PEG samples and the PEO sample of the largest M_w ($=1.60 \times 10^4$) are also isolated even in the aqueous solutions. From the results of dynamic light scattering measurements for the aqueous solution of the PEO sample with $M_w = 3.81 \times 10^3$ at 25.0 °C, there were detected two classes of scatterers having different sizes, i.e., the isolated chains and aggregates, the apparent hydrodynamic radius of the latter being *ca*. twenty times as large as that of the former.

Introduction

As is well known, polyoxyethylene (POE) is a typical nonionic water-soluble polymer at room temperature. Usually, POE having hydroxy groups at both chain ends is called poly(ethylene glycol) (PEG) and that having a methoxy group at one end and a hydroxy group at the other is called poly(ethylene oxide) (PEO). The difference in the one end group between PEG and PEO is immaterial for their dilute aqueous solution behavior if their molecular weight M is very large [1–3].

We have previously studied aqueous solution behavior of linear and random-branched poly(*N*-isopropylacrylamide) (PNIPA) having a hydrophobic diphenylmethyl group at one chain end and an isobutyronitrile group at almost every end, respectively [4]. Aqueous PNIPA solutions are apparently transparent at room temperature and become turbid above the cloud point near human body temperature, like as the lower-critical-solution-temperature miscibility behavior, although it is highly doubtful that the cloud-point curve in the aqueous PNIPA solutions directly corresponds to the binodal [4]. It has been shown for both linear and branched PNIPA of $M \sim 10^4$ that there exist some aggregates of PNIPA in aqueous solutions even at temperatures below the cloud point. Such aggregations may be regarded as arising from the hydrophobic chain ends and therefore are enhanced with decreasing M. It may be expected that this is also the case with PEO with the hydrophobic methoxy chain end in aqueous solution if its M becomes small.

In the present study, we therefore carry out static light scattering (SLS) measurements for both PEG and PEO of small M in water and also methanol at 25.0 °C. First, we determine the weight-average molecular weight M_w along with the second virial coefficient A_2 of PEG and PEO samples in methanol (good solvent). Then, the SLS behavior for PEG and PEO in water is compared with that in methanol. In anticipation of the results, it is found from the comparison that aggregates of large size are formed only for PEO with small M_w in water. Finally, dynamic light scattering (DLS) measurements are carried out for the aqueous PEO solution to examine the aggregation behavior, in some detail.

✉ Masashi Osa
mosa@auecc.aichi-edu.ac.jp

✉ Daichi Ida
ida@molsci.polym.kyoto-u.ac.jp

[1] Department of Polymer Chemistry, Kyoto University, Kyoto, Japan

[2] Department of Chemistry, Aichi University of Education, Kariya, Japan

Experimental procedure

Materials

Two PEG and three PEO test samples were used in this study. Each PEG test sample was the fraction separated by fractional precipitation using benzene as a solvent and isooctane as a precipitant from the commercial samples, Poly(ethylene glycol) average Mn 3,350 powder supplied by Sigma-Aldrich, Co. LLC (St. Louis, MO, USA) and Polyethylene Glycol 20,000 supplied by Wako Pure Chemical Industries, Ltd. (Osaka, Japan), respectively, with preliminary purification by reprecipitation from benzene solutions into *n*-hexane. The two of the PEO test samples were the fractions separated from the commercial samples P4109-EGOCH3 and P6274-EGOCH3, respectively, supplied by Polymer Source Inc. (Montreal, Quebec, Canada) with the preliminary purification, in the same manner as in the case of the PEG samples. The commercial PEO sample P4358-EGOCH3 supplied by Polymer Source, Inc. with the preliminary purification was adopted as the remaining PEO test sample. All of the test samples were freeze-dried from their benzene solutions after filtration through a Teflon membrane (Sumitomo Electric Industries, Ltd., Osaka, Japan) of pore size 1.0 μm. The samples were dried in a vacuum at *ca*. 50 °C for 12 h just before use.

In the first column of Table 1 are given the codes of all the samples so prepared. The values of the ratio of M_w to the number-average molecular weight M_n were determined from analytical gel permeation chromatography with a Shodex OHpak SB-804 HQ column (Showa Denko KK, Tokyo, Japan) connected to a PU-980 solvent delivery pump (JASCO Corporation, Tokyo, Japan) and a RI-8000 refractive index detector (Tosoh Corporation, Tokyo, Japan) using 0.2 M aqueous $NaNO_3$ solution as an eluent and seven standard POE samples ($M_w = 62-2.52 \times 10^5$) as reference standards. The M_w/M_n values so determined are 1.0_9, 1.1_1, 1.0_9, 1.0_9, and 1.3_5 for PEG3, PEG21, PEO4, PEO7, and PEO16, respectively. We note that the chemical structures of PEG3 and PEO4 were confirmed by ^{1}H nuclear magnetic resonance measurements in $CDCl_3$ at room temperature using an EX-400 spectrometer (JEOL, Ltd., Tokyo, Japan) at 399.8 MHz (details are omitted for simplicity).

Table 1 Results of LS measurements for poly(ethylene glycol) and poly(ethylene oxide) in methanol and water at 25.0 °C

Sample	In methanol at 25.0 °C		In water at 25.0 °C		
	$10^{-3}\ M_w$	$10^3 A_2$ (cm^3 mol/g^2)	$10^{-3}\ M_w$	$10^3 A_2$ (cm^3 mol/g^2)	$\langle S^2 \rangle^{1/2}$ (nm)
PEG3	3.46	1.9_0	3.51	2.9_5	
PEG21	21.2	1.2_5	21.6	1.6_1	
PEO4	3.81	1.9_2	33.8	0.5_6	$40._9$
PEO7	7.00	1.4_9	11.6	1.1_2	$17._4$
PEO16	16.0	1.2_4	16.8	1.6_7	

Methanol for SLS measurements was purified by distillation after refluxing over calcium hydride for *ca*. 6 h. Water used for SLS and DLS measurements was highly purified through a Simpli Lab water purification system of Merck Millipore, Co. (Billerica, MA, USA), its resistivity being 18.2 MΩ cm.

Static light scattering

SLS measurements were carried out for all PEG and PEO samples in both methanol and water at 25.0 °C, and M_w and A_2 were determined for each sample in both solvents. We note that only for PEO4 and PEO7 in water, it was possible to determine the mean-square radius of gyration $\langle S^2 \rangle$ because of the existence of aggregates of large size, as described later. A Fica 50 light-scattering photometer (Saint Denis, France) was used for all the measurements with vertically polarized incident light of wavelength $\lambda_0 = 436$ nm. To calibrate the apparatus, the intensity of light scattered from pure benzene was measured at 25.0 °C at a scattering angle of 90°, where the Rayleigh ratio $R_{Uu}(90°)$ of pure benzene was taken as 46.5×10^{-6} cm^{-1} [5]. The depolarization ratio ρ_u of pure benzene at 25.0 °C was determined to be 0.41 ± 0.01. Scattered intensity was measured at six different concentrations and at scattering angles θ ranging from 30 to 142.5°, and then was converted to the excess unpolarized components ΔR_{Uv} of the reduced scattered intensity by using the scattered intensity from the solvents. The obtained data were treated by using the Berry square-root plot [6]. For all samples, corrections for optical anisotropy were unnecessary since the degree of depolarization was negligibly small.

The most concentrated methanol and aqueous solutions of each sample were prepared gravimetrically and made homogeneous by continuous stirring at room temperature for 2 days, with preliminary stirring at 50 °C for 1 h for the methanol solutions. Almost all the methanol and aqueous solutions were optically purified by filtration through two layers of a Teflon membrane (Sumitomo Electric Industries, Ltd.) of pore size 0.10 μm and those of a poly(vinylidene difluoride) membrane (Merck Millipore, Co.) of pore size 0.10 μm, respectively, except for the methanol solutions of PEG21 and PEO16 which were purified by filtration through only the (single) Teflon membrane of pore size 0.10 μm. The solutions of lower concentrations were obtained by successive dilution. The weight concentrations of the test solutions were converted to the polymer mass concentrations c using the densities ρ_0 of methanol and water. For ρ_0 of methanol and water at 25.0 °C, we used the

literature values 0.7866 g/cm^3 [7] and 0.99704 g/cm^3 [8], respectively.

The refractive index increment $\partial n/\partial c$ was measured at the wavelength of 436 nm using a differential refractometer DR-1 (Shimadzu, Co., Kyoto, Japan). The values of $\partial n/\partial c$ in methanol at 25.0 °C were determined to be 0.148, 0.150, 0.152, 0.151, and 0.151 cm^3/g for the samples PEG3, PEG21, PEO4, PEO7, and PEO16, respectively, and those in water at 25.0 °C were 0.138, 0.139, 0.139, 0.139, and 0.140 cm^3/g for the respective samples in the same order.

For the refractive index n_0 of methanol and water at 25.0 °C and at the wavelength of 436 nm, we used the literature values 1.3337 and 1.3390, respectively [7].

Dynamic light scattering

DLS measurements were carried out for the aqueous solution of the sample PEO4 at 25.0 °C, which was found in the SLS measurements described above to form aggregates. For the DLS measurements, a BI-200SM light scattering goniometer (Brookhaven Instruments, Co., New York, USA) was used with vertically polarized incident light of $\lambda_0 =$ 532 nm from a Millenia Pro 2s Nd:YVO_4 laser (Spectra-Physics, Inc., Santa Clara, CA, USA). The photomultiplier tube used was a 9893B/350 model (EMI Group, Ltd., London, UK), whose output was processed by a BI-9000AT Digital Correlator (Brookhaven Instruments, Co.). An electric shutter was attached to the original detector alignment to automatically monitor the dark count. The normalized autocorrelation function $g^{(2)}(t)$ of the scattered light intensity $I(t)$ at time t along with the time-averaged intensity $\overline{I}$ were measured for the aqueous solution at θ ranging from 20 to 120°. To calibrate the apparatus, which is necessary for an evaluation of ΔR_{Uv} from $\overline{I}$ for each aqueous solution, $\overline{I}$ was also measured for pure toluene at 25.0 °C and at $\theta =$ 90°, where $R_{\mathrm{Uv}}(90°)$ of pure toluene was taken as 27.4×10^{-6} cm^{-1} [9].

The aqueous solutions of $c = 1.01 \times 10^{-2}$ and 1.92×10^{-2} g/cm^3 were prepared in the same manner as in the case of the SLS measurements. The value of n_0 of water at $\lambda_0 = 532$ nm and at 25.0 °C was estimated to be 1.3345 by a linear interpolation of the plot of n_0 against λ_0^{-2} with the literature values [7] 1.3390 and 1.3340 of n_0 of water at 25.0 °C and at $\lambda_0 = 436$ and 546 nm, respectively. We used the value 0.890 cP of the viscosity coefficient η_0 of water at 25.0 °C [10]. For later use, the viscosity coefficient η was determined for the aqueous solutions of the sample PEO4 at $c = 1.01 \times 10^{-2}$ and 1.92×10^{-2} g/cm^3 and at 25.0 °C by the use of a capillary viscometer with the use of the above-mentioned value of η_0 of water at the temperature. The values of η so determined are 1.01 and 1.13 cP for the solutions with $c = 1.01 \times 10^{-2}$ and 1.92×10^{-2} g/cm^3, respectively.

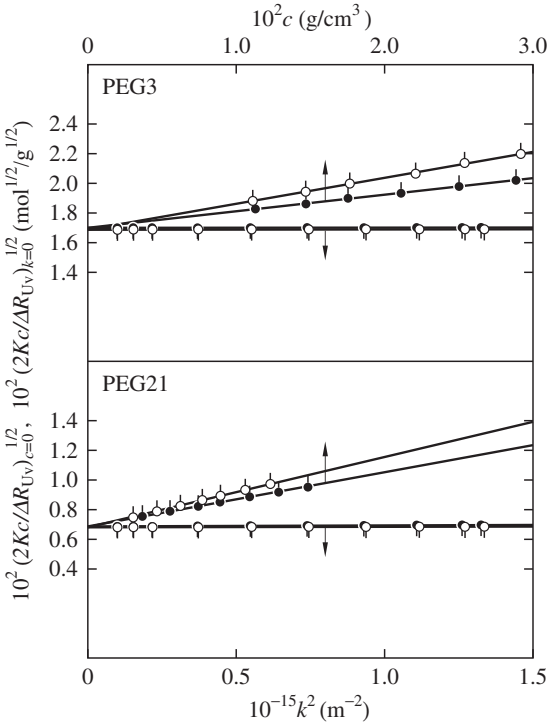

Fig. 1 Plots of $(2Kc/\Delta R_{\mathrm{Uv}})_{k=0}^{1/2}$ (pip up) and $(2Kc/\Delta R_{\mathrm{Uv}})_{c=0}^{1/2}$ (pip down) against c and k^2, respectively, for the PEG samples PEG3 and PEG21 in water (○) and methanol (●) at 25.0 °C

Results and discussion

Static light scattering

The data of ΔR_{Uv} so obtained for each solution were treated by using the Berry square-root plot [6] in the form of $(2Kc/\Delta R_{\mathrm{Uv}})^{1/2}$, where K is the optical constant defined by

$$K = \frac{2\pi^2 n_0^2}{\lambda_0^4 N_{\mathrm{A}}} \left(\frac{\partial n}{\partial c}\right)^2 \tag{1}$$

with N_{A} the Avogadro constant. The plots of $(2Kc/\Delta R_{\mathrm{Uv}})^{1/2}$ against c and the square of the magnitude k of the scattering vector, defined by $k = (4\pi n_0/\lambda_0)\sin(\theta/2)$, for each solution followed by the corresponding straight lines, and then, may be extrapolated to $k = 0$ and $c = 0$, respectively, to evaluate the corresponding limiting values $(2Kc/\Delta R_{\mathrm{Uv}})_{k=0}^{1/2}$ as a function of c and $(2Kc/\Delta R_{\mathrm{Uv}})_{c=0}^{1/2}$ as a function of k (or k^2).

Figure 1 shows plots of $(2Kc/\Delta R_{\mathrm{Uv}})_{k=0}^{1/2}$ (pip up) and $(2Kc/\Delta R_{\mathrm{Uv}})_{c=0}^{1/2}$ (pip down) against c and k^2, respectively, for PEG3 and PEG21 in water (unfilled circle) and methanol (filled circle) at 25.0 °C. For each sample in both solvents, the two kinds of plots follow the corresponding straight lines in the ranges of c and k^2 examined and may be extrapolated to obtain the common intercept. The weight-average molecular weight M_{w} and second virial coefficient A_2 may then be determined from the common intercept and

the slope of the line for the plots of $(2Kc/\Delta R_{\mathrm{Uv}})_{k=0}^{1/2}$ against c, respectively. The values of M_{w} and A_2 so determined are given in the second and third columns, respectively, of Table 1 for the methanol solutions and in the fourth and fifth columns, respectively, of the table for the aqueous solutions. We note that the mean-square radius of gyration $\langle S^2 \rangle$ could not be precisely determined since there is no appreciable dependence of $(2Kc/\Delta R_{\mathrm{Uv}})_{c=0}^{1/2}$ on k.

The value of A_2 for each sample in water is definitely larger than that in methanol, indicating that water may be regarded as a better solvent than methanol for the PEG samples. For each sample, both the M_{w} values in water and methanol agree well with each other within experimental errors. This fact along with the weak dependence of $(2Kc/\Delta R_{\mathrm{Uv}})_{c=0}^{1/2}$ on k indicates that PEG3 and PEG21 are isolated in both water and methanol at 25.0 °C, similar to the case of PEG and/or PEO with large M, as mentioned in Introduction [1–3].

Figure 2 shows similar plots for PEO4, PEO7, and PEO16 in water (unfilled circle) and methanol (filled circle) at 25.0 °C. The behavior of the plots for all of the samples in methanol and PEO16 in water is essentially same as that for the PEG samples. For PEO4 and PEO7, however, the common intercept for the aqueous solutions is appreciably smaller than that for the methanol solutions and the data of $(2Kc/\Delta R_{\mathrm{Uv}})_{c=0}^{1/2}$ follow the straight line of definitely positive slope. The values of M_{w} and A_2 determined in the same manner as in the case of the PEG samples are given in the second and third columns, respectively, of Table 1 for the methanol solutions and in the fourth and fifth columns, respectively, of the table for the aqueous solutions. In the sixth column of the table, there are also given the values of $\langle S^2 \rangle^{1/2}$ estimated from the slope of the plots of $(2Kc/\Delta R_{\mathrm{Uv}})_{c=0}^{1/2}$ against k^2 for PEO4 and PEO7 in water.

The values of M_{w} for PEO4 and PEO7 in water are much larger than those in methanol, while the values of M_{w} for PEO16 in water and methanol agree fairly with each other. [Strictly, the value in water is slightly (5%) larger than that in methanol.] This fact along with the dependence of $(2Kc/\Delta R_{\mathrm{Uv}})_{c=0}^{1/2}$ on k clearly indicates that there exist some aggregates of large size, in addition to isolated PEO chains, in the aqueous solutions of PEO4 and PEO7 at 25.0 °C.

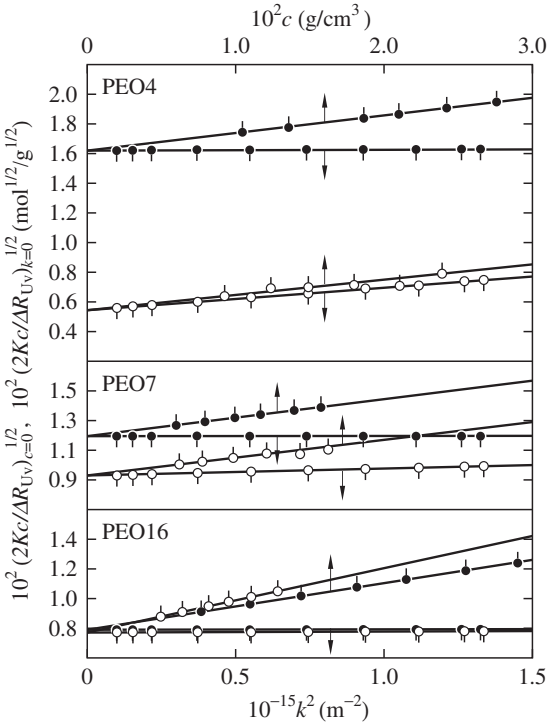

Fig. 2 Plots of $(2Kc/\Delta R_{\mathrm{Uv}})_{k=0}^{1/2}$ (pip up) and $(2Kc/\Delta R_{\mathrm{Uv}})_{c=0}^{1/2}$ (pip down) against c and k^2, respectively, for the PEO samples PEO4, PEO7, and PEO16 in water (○) and methanol (●) at 25.0 °C

Dynamic light scattering

In the last section, it was shown that some aggregates of large size are formed in the aqueous solutions of the samples PEO4 and PEO7 at 25.0 °C, while all PEG and PEO samples are isolated in methanol, and the PEG samples and the PEO sample of the largest M_{w} (PEO16) are also isolated even in water. We then pursue further the aggregation behavior of PEO in water on the basis of the results of DLS measurements for the aqueous solution of the sample PEO4, which exhibits the most remarkable aggregation behavior as seen in the SLS results (Fig. 2).

Figure 3, as a typical example, shows plots of $[g^{(2)}(t) - 1]^{1/2}$ against the logarithm of t at $\theta = 20°$ and $c = 1.92 \times 10^{-2}$ g/cm^3 for the sample PEO4 in water at 25.0 °C. The unfilled circles represent the experimental data, and the

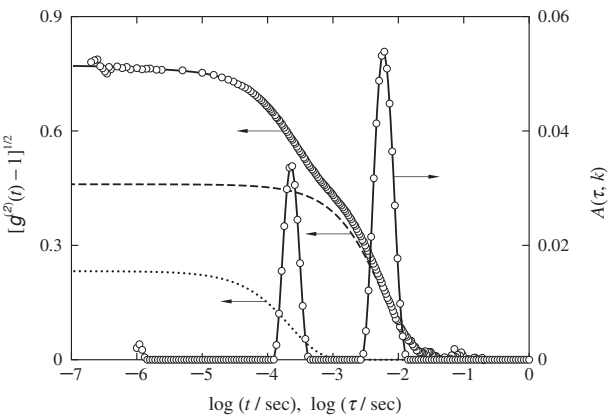

Fig. 3 Plots of $[g^{(2)}(t) - 1]^{1/2}$ against the logarithm of t and those of $A(\tau, k)$ against the logarithm of τ at $\theta = 20°$ and $c = 1.92 \times 10^{-2}$ g/cm^3 for the sample PEO4 in water at 25.0 °C. The unfilled circles represent the experimental values and the solid curves connect smoothly the data points. The dotted and dashed curves represent the values of the contributions of the fast and slow modes, respectively, to $[g^{(2)}(t) - 1]^{1/2}$ (see text)

solid curve connects the data smoothly. The data do not seem to follow a single exponential decay. This is also the case with the data in the whole range of θ examined for both $c = 1.01 \times 10^{-2}$ and 1.92×10^{-2} g/cm^3.

As in a previous study [4], by the use of the FORTRAN program package CONTIN [11], we decomposed $[g^{(2)}(t) - 1]^{1/2}$ at a given k into a series of exponential-decay functions as follows,

$$\left[g^{(2)}(t) - 1\right]^{1/2} = \sum_{i=1}^{n_f} A(\tau_i, k) e^{-t/\tau_i}, \tag{2}$$

where τ_i ($i = 1, 2, \ldots, n_f$) is the ith relaxation time and $A(\tau_i, k)$ is the amplitude of the ith component e^{-t/τ_i}, the latter quantity as a function of the relaxation time τ having the meaning of the distribution of τ. In practice, we adopted $n_f = 150$ and distributed τ_i at regular intervals in the logarithmic scale over the range from 1 μs to 1 s.

In Fig. 3, the data of $A(\tau, k)$ so obtained, corresponding to the data of $[g^{(2)}(t) - 1]^{1/2}$ described above, are also plotted against the logarithm of τ, represented by the unfilled circles with the solid curve connecting them smoothly. The quantity $A(\tau, k)$ as a function of τ is clearly bimodal, indicating that there are two classes of scatterers with different sizes. The class with larger τ (=10^{-3}–10^{-2} s) may be considered to be large aggregates, and the other class ($\tau = 10^{-4}$–10^{-3} s) seems to correspond to isolated PEO chains. Such behavior of $A(\tau, k)$ was observed over the whole range of θ examined for both $c = 1.01 \times 10^{-2}$ and 1.92×10^{-2} g/cm^3. It is seen that there exists a threshold value of τ which divides the distribution of $A(\tau,k)$ into two modes: one is called the fast mode, which is a set of relaxation times (τ_i) smaller than the threshold value, and the other is called the slow mode otherwise. We may then calculate $\left[g^{(2)}(t) - 1\right]_{\alpha}^{1/2}$ for the α modes ($\alpha =$ fast, slow) using τ_i and $A(\tau_i, k)$ belonging to the α mode as follows,

$$\left[g^{(2)}(t) - 1\right]_{\alpha}^{1/2} = \sum_{\tau_i \in \alpha \text{ mode}} A(\tau_i, k) e^{-t/\tau_i} \ (\alpha = \text{fast, slow}). \tag{3}$$

In Fig. 3, the values of $\left[g^{(2)}(t) - 1\right]_{\text{fast}}^{1/2}$ and $\left[g^{(2)}(t) - 1\right]_{\text{slow}}^{1/2}$ are also plotted against the logarithm of t, represented by the dotted and dashed curves, respectively. The decay of $[g^{(2)}(t) - 1]^{1/2}$ itself seems to be well reproduced by the summation of $\left[g^{(2)}(t) - 1\right]_{\text{fast}}^{1/2}$ and $\left[g^{(2)}(t) - 1\right]_{\text{slow}}^{1/2}$.

Now, assuming that the solution includes only a small amount of aggregates, interactions between them may be neglected, and the lifetime of each aggregate is much longer than its translational relaxation time, the mutual diffusion coefficient D_{fast} of the isolated chains and z-average translational diffusion coefficient D_{slow} of the aggregates may be given by [9]

$$D_{\alpha} = \lim_{k \to 0} \Gamma_{\alpha}/k^2 \ (\alpha = \text{fast, slow}) \tag{4}$$

with

$$\Gamma_{\alpha} = \sum_{\tau_i \in \alpha \text{ mode}} \tau_i^{-1} A(\tau_i, k) \Big/ \sum_{\tau_i \in \alpha \text{ mode}} A(\tau_i, k) (\alpha = \text{fast, slow}). \tag{5}$$

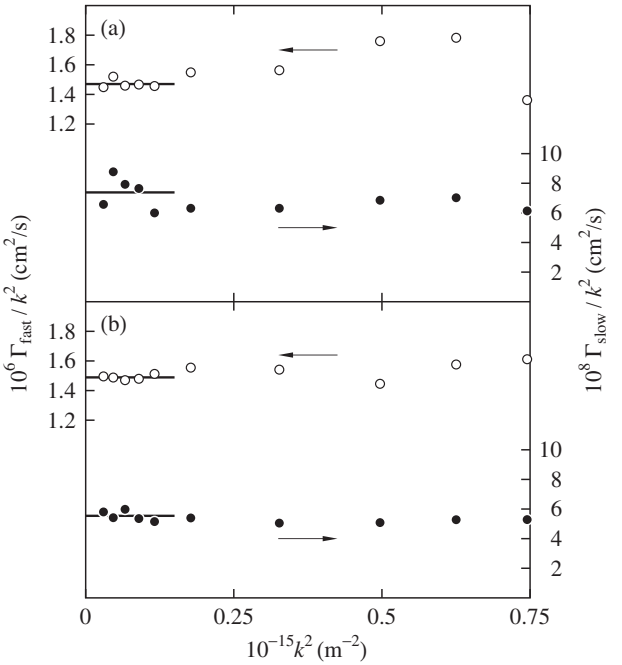

Fig. 4 Plots of Γ_{α}/k^2 against k^2 for the sample PEO4 in water at 25.0 °C with $c = 1.01 \times 10^{-2}$ (**a**) and 1.92×10^{-2} g/cm^3 (**b**). The unfilled and filled circles represent the experimental values of Γ_{fast}/k^2 and Γ_{slow}/k^2, respectively. The solid horizontal line segments represent the corresponding mean of the Γ_{α}/k^2 values in the range of θ from 20° to 40°

Figure 4 shows plots of the values of Γ_{α}/k^2 against k^2 for the sample PEO4 in water at 25.0 °C with $c = 1.01 \times 10^{-2}$ (a) and 1.92×10^{-2} g/cm^3 (b). The unfilled and filled circles represent the values of Γ_{fast}/k^2 and Γ_{slow}/k^2, respectively. The mean of Γ_{α}/k^2 in the range of θ from 20° to 40°, indicated by the solid horizontal line segment, was adopted as the limiting value of Γ_{α}/k^2 in the limit of $k \to 0$ or D_{α} for each case, although the data points of Γ_{slow}/k^2 for $c = 1.01 \times 10^{-2}$ g/cm^3 are somewhat scattered. The values of D_{fast} so evaluated are $1.4_7 \times 10^{-6}$ and $1.4_9 \times 10^{-6}$ cm^2/s for $c = 1.01 \times 10^{-2}$ and 1.92×10^{-2} g/cm^3, respectively, and also, those of D_{slow} are estimated to be $7.3_8 \times 10^{-8}$ and $5.5_4 \times 10^{-8}$ cm^2/s for $c = 1.01 \times 10^{-2}$ and 1.92×10^{-2} g/cm^3, respectively.

From the values of D_{α} so obtained, we define the apparent hydrodynamic radius $R_{\text{H,ap},\alpha}$ (at finite concentration) as follows,

$$R_{\text{H,ap},\alpha} = k_{\text{B}} T / 6\pi\eta_{\alpha} D_{\alpha} \ (\alpha = \text{fast, slow}), \tag{6}$$

Table 2 Values of $R_{H,ap,\alpha}$ (α = fast, slow), $\langle S^2 \rangle_{ap,slow}^{1/2}$, and $\rho_{ap,slow}$ at finite mass concentration c for the sample PEO4 in water at 25.0 °C

$10^2\ c$ (g/cm^3)	$R_{H,ap,fast}$ (nm)	$R_{H,ap,slow}$ (nm)	$\langle S^2 \rangle_{ap,slow}^{1/2}$ (nm)	$\rho_{ap,slow}$
1.01	1.6_7	$29._3$	$29._8$	1.0_2
1.92	1.6_5	$34._8$	$29._0$	0.83_3

where η_{fast} and η_{slow} are the viscosity coefficients of fluids around the isolated chains and aggregates. The coefficients η_{fast} and η_{slow} may be set equal to the solvent viscosity coefficient η_0 and solution viscosity coefficient η, respectively [9]. In the second and third column of Table 2 are given the values of $R_{H,ap,fast}$ and $R_{H,ap,slow}$, respectively, at $c = 1.01 \times 10^{-2}$ and 1.92×10^{-2} g/cm^3 calculated from Eq. (6) with the above-mentioned values of D_α and η_α. The radii $R_{H,ap,fast}$ and $R_{H,ap,slow}$ are almost independent of c. The value of $R_{H,ap,slow}$ at each c is *ca.* twenty times as large as the corresponding value of $R_{H,ap,fast}$. It may then be concluded that the slow mode reflects the translational motion of the aggregates of large size.

To clarify what the α mode (α = fast, slow) reflects, the data of the contribution $\Delta R_{Uv,\alpha}(k)$ from the α mode component to $\Delta R_{Uv}(k)$ determined from the time-averaged scattering intensity $\overline{I}(k)$ were analyzed. The contribution $\Delta R_{Uv,\alpha}(k)$ may be given by [9]

$$\Delta R_{Uv,\alpha}(k) = \Delta R_{Uv}(k) \sum_{\tau_i \in \alpha \text{ mode}} A(\tau_i, k) / \sum_{i=1}^{n_f} A(\tau_i, k). \quad (7)$$

For each c, $[2Kc/\Delta R_{Uv,fast}(k)]^{1/2}$, calculated from Eq. (7) (using the $\partial n/\partial c$ value at $\lambda_0 = 436$ nm, for convenience), was found to be almost independent of k, and then the limiting value $[2Kc/\Delta R_{Uv,fast}(0)]^{1/2}$ was determined as the mean of $[2Kc/\Delta R_{Uv,fast}(k)]^{1/2}$ at each θ. The values of $[2Kc/\Delta R_{Uv,fast}(0)]^{1/2}$ so determined are $1.8_3 \times 10^{-2}$ and $2.0_6 \times 10^{-2}$ mol$^{1/2}$/g$^{1/2}$ for $c = 1.01 \times 10^{-2}$ and 1.92×10^{-2} g/cm^3, respectively. Although only the two data points were obtained, the weight-average molecular weight $M_{w,fast}$ of the fast mode component was roughly estimated by extrapolation of $[2Kc/\Delta R_{Uv,fast}(0)]^{1/2}$ to $c = 0$ on the assumption that the weight fraction of the fast mode component in the total solute polymer is unity [9]. The $M_{w,fast}$ value so estimated is $(4.0 \pm 0.9) \times 10^3$, which agrees fairly with M_w of the PEO4 sample determined in methanol at 25.0 °C (see Table 1). We may then conclude that the fast mode reflects the translational motion of the isolated chains.

For each c, we also estimated the apparent mean-square radius of gyration $\langle S^2 \rangle_{ap,slow}$ of the aggregates (at finite c) from [9]

$$\left[\Delta R_{Uv,slow}(0)/\Delta R_{Uv,slow}(k)\right]^{1/2} = 1 + \frac{1}{6}\langle S^2 \rangle_{ap,slow} k^2 + \cdots. \quad (8)$$

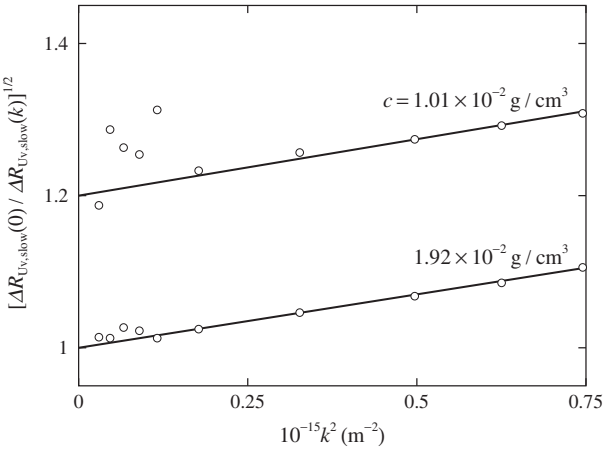

Fig. 5 Plots of $[\Delta R_{Uv,slow}(0)/\Delta R_{Uv,slow}(k)]^{1/2}$ against k^2 for the sample PEO4 in water at 25.0 °C with $c = 1.01 \times 10^{-2}$ and 1.92×10^{-2} g/cm^3. The unfilled circles represent the experimental values of $[\Delta R_{Uv,slow}(0)/\Delta R_{Uv,slow}(k)]^{1/2}$ with the corresponding best-fit straight lines. The data points and line for $c = 1.01 \times 10^{-2}$ g/cm^3 are shifted upward by 0.2

Figure 5 shows plots of $[\Delta R_{Uv,slow}(0)/\Delta R_{Uv,slow}(k)]^{1/2}$ against k^2 for PEO4 in water at 25.0 °C with $c = 1.01 \times 10^{-2}$ and 1.92×10^{-2} g/cm^3. The unfilled circles represent the experimental values of $[\Delta R_{Uv,slow}(0)/\Delta R_{Uv,slow}(k)]^{1/2}$, the data points for $c = 1.01 \times 10^{-2}$ g/cm^3 being shifted upward by 0.2. Although the data points are somewhat scattered in the range of small k ($k^2 \lesssim 0.12 \times 10^{15}$ m^{-2}) for each c, the values of $\langle S^2 \rangle_{ap,slow}$ were evaluated from the slope of the corresponding best-fit straight lines following Eq. (8). The values of $\langle S^2 \rangle_{ap,slow}^{1/2}$ so evaluated are given in the fourth column of Table 2. The radius $\langle S^2 \rangle_{ap,slow}^{1/2}$ is *ca.* 30 nm irrespective of c. [Note that $\langle S^2 \rangle_{ap,slow}^{1/2}$ is smaller than the $\langle S^2 \rangle^{1/2}$ value at infinite dilution, as determined for the aqueous solution of PEO4 by SLS measurements (see Table 1).] In the fifth column of Table 2 are also given the values of the ratio $\rho_{ap,slow}$ of $\langle S^2 \rangle_{ap,slow}^{1/2}$ to $R_{H,ap,slow}$. The $\rho_{ap,slow}$ values are larger than the value 0.775 of the ratio ρ of $\langle S^2 \rangle^{1/2}$ to the hydrodynamic radius (at infinite dilution) for rigid spheres with uniform density and smaller than the value 1.2–1.5 of ρ for random coils [12]. This indicates that the aggregates of PEO4 in water at finite c are looser than rigid spheres with uniform density and denser than random coils.

Finally, we make some comments on the shape and structure of the aggregates formed in the aqueous PEO solutions. In a series of systematic and comprehensive experimental studies by Einaga et al. [13, 14] of the shape and structure of wormlike micelles of nonionic surfactants, polyoxyethylene alkyl ethers $H(CH_2)_i(OCH_2CH_2)_jOH$ (C_iE_j, $i = 10$–18, $j = 5$–8), formed in aqueous solutions, it

has been shown that with decreasing i, the contour length of the wormlike micelles decreases without appreciable change in the diameter of the cross section of the micelles. This indicates that for much smaller i, spherical micelles of a core–shell structure may be formed. Considering the fact that PEO corresponds to C_1E_j along with the values of $\rho_{ap,slow}$, it may be concluded that the aggregates of PEO in aqueous solutions of finite c are also spherical and have a core–shell structure.

Concluding remarks

SLS measurements were carried out in water and methanol at 25.0 °C for two kinds of POE samples of low M_w (3×10^3–2×10^4): PEG having hydroxy groups at both ends and PEO having a methoxy group at one end and a hydroxy group at the other. All the PEG and PEO samples were shown to be isolated in methanol solutions. In water, on the other hand, it was found that the PEO samples with $M_w = 3.81 \times 10^3$ and 7.00×10^3 form aggregates of large size, while all the PEG samples and the PEO sample of the largest M_w ($=1.60 \times 10^4$) were isolated as in the cases of their methanol solutions.

DLS measurements were also carried out in water at 25.0 °C for the PEO sample with $M_w = 3.81 \times 10^3$. It was found that there exist two classes of scatterers of different sizes in aqueous solution: one corresponds to isolated PEO chains, and the other to aggregates. The apparent hydrodynamic radius of the aggregates was shown to be *ca.* twenty times as large as that for the isolated chains. Considering the indication that spherical micelles of a core–shell structure may be formed in aqueous solutions of polyoxyethylene alkyl ethers with small alkyl chain length, the aggregates of PEO in aqueous solution also seem to be spherical and have a core–shell structure.

It is pertinent to make some comments on the formation of polymer aggregates in good solvents. Although POE has been usually considered to be dissolved or isolated in water, the present results indicate that POE having hydrophobic chain ends with small M may form aggregates of large size even in water because of the so-called hydrophobic interactions between the hydrophobic parts as in the cases of PNIPA [4] and amphiphilic copolymers (including amphiphilic polyelectrolytes) [15] in aqueous solutions. Similar situations have been recognized also for good-solvent systems composed of hydrophobic polymers and solvents of low polarity, such as polystyrene in tetrahydrofuran [9, 16] and poly(*n*-hexyl isocyanate) in *n*-hexane [9, 17]. For the precise characterization of polymers in solutions, we should always pay attention to the formation of aggregates.

Compliance with ethical standards

Conflict of interest The authors declare that they have no competing interests.

References

1 Devenand K, Selser JC. Asymptotic behavior and long-range interactions in aqueous solutions of poly(ethylene oxide). Macromolecules 1991;24:5943–7.
2 Kinugasa S, Nakahara H, Fudagawa N, Koga Y. Aggregative behavior of poly(ethylene oxide) in water and methanol. Macromolecules 1994;27:6889–92.
3 Kawaguchi S, Imai G, Suzuki J, Miyahara A, Kitano T, Ito K. Aqueous solution properties of oligo- and poly(ethylene oxide) by static light scattering and intrinsic viscosity. Polym 1997;38:2885–91.
4 Kawaguchi T, Kobayashi K, Osa M, Yoshizaki T. Is a cloud-point curve in aqueous poly(*N*-isopropylacrylamide) solution binodal? J Phys Chem B 2009;113:5440–7.
5 Deželić Gj, Vavra J. Angular dependence of the light scattering in pure liquids. Croat Chem Acta 1966;38:35–47.
6 Berry GC. Thermodynamic and conformational properties of polystyrene. I. Light-scattering studies on dilute solutions of linear polystyrenes. J Chem Phys 1966;44:4550–64.
7 Johnson BL, Smith J. In: Huglin MB, editor. Light scattering from polymer solutions. London: Academic Press; 1972. Ch. 2.
8 Spieweck F, Bettin H. Review: solid and liquid density determination. Tech Mess 1992;59:285–92.
9 Kanao M, Matsuda Y, Sato T. Characterization of polymer solutions containing a small amount of aggregates by static and dynamic light scattering. Macromolecules 2003;36:2093–102.
10 National Astronomical Observatory of Japan, editor. Rika Nenpyo, Tables for scientific data (Maruzen, Tokyo, 2003).
11 Provencher SW. A constrained regularization method for inverting data represented by linear algebraic or integral equations. Comput Phys Commun 1982;27:213–27.
12 Yamakawa H, Yoshizaki T. Helical wormlike chains in polymer solutions. 2nd ed. Springer: Berlin; 2016.
13 Einaga Y. Wormlike micelles of polyoxyethylene alkyl ethers C_iE_j. Polym J 2009;41:157–73.
14 Yoshimura S, Shirai S, Einaga Y. Light-scattering characterization of the wormlike micelles of hexaoxyethylene dodecyl $C_{12}E_6$ and hexaoxyethylene tetradecyl $C_{14}E_6$ ethers in dilute aqueous solution. J Phys Chem B 2004;108:15477–87.
15 Hashidzume A, Kawaguchi A, Tagawa A, Hyoda K, Sato T. Synthesis and structural analysis of self-associating amphiphilic statistical copolymers in aqueous media. Macromolecules 2006;39:1135–43.
16 Gan YSJ, Frongois J, Guenet J-M. Enhanced low-angle scattering from moderately concentrated solutions of atactic polystyrene and its relation to physical gelation. Macromolecules 1986;19:173–8.
17 Sato T, Kanao M. Characterization of aggregating polymer solutions by light scattering: *n*-hexane solution of poly(*n*-hexyl isocyanate). Koubunshi Ronbunshu 2003;60:158–68.